Indian Journal of Pure & Applied Physics
Vol. 64, February 2026, pp. 221-231
DOI: 10.56042/ijpap.v64i2.26109

Integrating Demand Response and Solar PV in Indian Coal Power Plants: A Hippopotamus Optimization Approach to Emission Mitigation

Vivek Saxena[a], Vikrant Shokeen[b], Shyamsundar[c], Saibal Manna[a], Bhupender Sharma[a] & Nishant Kumar[d*]

[a]Department of Electrical & Computer Engineering, ABES Engineering College, Ghaziabad 201 009, India
[b]Department of Computer Science Engineering, Maharaja Surajmal Institute of Technology, Janakpuri 110 058, India
[c]Department of Electrical Engineering, Government Engineering College Gopalganj, Bihar 841 501, India
[d]Department of Electrical Engineering, B K Birla Institute of Engineering & Technology, Pilani 333 031, India

Received: 1st December 2025; accepted: 5th January 2026

Coal-fired electricity generation remains a dominant global source of greenhouse gas emissions, contributing approximately 15.22 billion metric tons of CO_2 in 2022. This study addresses the urgent need for decarbonization within the Indian coal-based power sector by examining the coordinated use of demand response (DR) strategies and optimally integrated solar photovoltaic (PV) systems. Solar PV is considered as a strategic complementary resource capable of reducing the dependence on conventional coal-fired units while enhancing clean distributed generation. The optimal siting and sizing of PV installations are determined using the Hippopotamus Optimization (HO) algorithm, which incorporates solar irradiance availability, temporal load patterns, and the emission intensity of coal-based supply. The proposed framework aims to increase renewable energy penetration, reduce technical losses, and achieve significant CO_2 mitigation while addressing solar intermittency and dynamic demand variations. Simulation results obtained on the IEEE 33-bus distribution system indicate that coordinated DR–PV integration leads to substantial reductions in peak demand, system losses, and up to 30.79 % reduction in CO_2 emissions compared to the base case. These findings highlight the effectiveness of combining renewable deployment with demand-side measures in achieving a sustainable, efficient, and environmentally responsible energy transition, offering valuable guidance for policymakers and utility planners engaged in coal-sector decarbonization.

Keywords: Atmospheric pollution, Demand response, Hippopotamus optimization, Indian power plant, Renewable energy

1 Introduction

Electricity forms the backbone of modern society, supporting residential activities, industrial production, and large-scale infrastructural development. Although global power generation draws from a diversified energy mix including renewable sources such as solar, wind, and hydropower, alongside conventional resources such as coal, natural gas, and nuclear fuels thermal generation remains a dominant source of greenhouse gas emissions. Coal-fired power plants, in particular, are among the most carbon-intensive technologies, underscoring the urgent need for technological and operational measures to mitigate their environmental footprint[1-4].

China exemplifies this challenge, where coal continues to dominate the national energy structure and contributes nearly 40 % of annual CO_2 emissions. In response, several studies have sought to enhance emission monitoring, prediction, and mitigation strategies. The authors introduced an RBF neural network-based framework to improve the accuracy of emission estimation from coal-fired stations, overcoming the limitations of conventional computational models[5]. The researchers further proposed source–network–load evaluation indicators aimed at supporting low-carbon transformation of captive coal power plants through systematic performance assessment[6].

Retrofitting existing thermal plants has also been explored as a viable pathway. Samanta *et al*., for instance, demonstrated that a partial repowering strategy for a 250 MW coal-fired unit could deliver up to 26.5 % CO_2 emission reduction and significant efficiency gains[7]. Broader assessments by the authors reveal that China's power sector could achieve emission reductions exceeding 265 Mt CO_2eq through structural optimization and expanded renewable integration[8].

Renewable energy deployment remains central to this transition. Studies involving solar farms and molten carbonate fuel cells show considerable potential in enhancing energy output while reducing

*Corresponding author: E-mail: krnishant125@gmail.com

environmental impacts[9]. Complementary advancements in waste heat recovery and chemical absorption technologies have demonstrated meaningful gains in CO_2 capture efficiency[10]. Nevertheless, the authors emphasized the continuing need for innovation in clean coal technologies, particularly within the context of stringent European climate policies[11].

Within future-ready smart grid architectures, distributed generation (DG) and DR are emerging as indispensable components. Renewable DG units including solar PV, wind turbines, small hydropower, and biomass systems offer environmentally sustainable alternatives, whereas non-renewable DG technologies, such as fuel cells and gas turbines, are constrained by resource limitations. Optimal siting and sizing of DG depend on network load characteristics, solar irradiation availability, and distribution network hosting capacity. DR programs, in which consumers modify their demand in response to price or incentive signals, contribute additional benefits such as peak load reduction, increased reliability, and deferred network reinforcement[12, 13].

Recent work demonstrates the synergistic advantages of integrating DR with solar PV within distribution networks, leading to improved PV utilization, enhanced voltage performance, and reduced system-level stress[14, 15]. As energy demand continues to rise amid tightening environmental constraints, DG technologies offer cost-efficient, flexible, and scalable pathways for achieving low-carbon development[16].

Accurate prediction of PV power generation is also essential for system planning and operational reliability. Machine learning and hybrid forecasting models leveraging real-time measurements and advanced analytical techniques have shown strong potential for both short-term and long-term PV output forecasting[17].

The role of DR and DG in advancing sustainable distribution networks has been widely recognized[18], alongside the importance of advanced optimization strategies for efficient DG integration[19, 20]. Given that approximately 70 % of global greenhouse gas emissions originate from the energy sector primarily through coal combustion the strategic deployment of low-emission DG technologies is critical for reducing dependence on thermal power plants[21].

In the Indian context, the growth of coal-based and hydro-based generation has slowed in recent years, further highlighting the need to integrate DR and solar PV with existing coal infrastructure to curb CO_2 emissions. According to the Central Electricity Authority[22], coal-fired power plants in India emit approximately 0.975 t CO_2/MWh, reinforcing the urgency of accelerating renewable DG adoption and developing smart, carbon-conscious operational frameworks[23]. Table 1 elaborate the comparative summary of the related literature.

Table 1 — Comparative summary of related literature

Ref.	Focus	Approach	Key Outcome	Limitation	Advancement in This Work
5	Emission estimation	RBF neural network	Accurate CO_2 estimation	No mitigation	Enables emission reduction, not just estimation
6	Coal plant assessment	Source–network–load indicators	Performance evaluation	No optimization	Adds optimization-based PV integration
7	Coal plant retrofit	Partial repowering	26.5% CO_2 reduction	High capital cost	Uses scalable DG–DR solutions
8	Sector-level planning	Structural optimization	Large CO_2 reduction potential	Macro-level only	Provides network-level analysis
9	Hybrid renewables	Solar + fuel cells	Improved efficiency	Complex, costly	Focuses on practical solar PV
10	CO_2 capture	WHR, absorption	Better capture efficiency	Tech-intensive	Uses operational grid measures
12, 13	Demand response	Price/incentive-based DR	Peak reduction	Low emission impact	Quantifies DR–PV emission benefits
14, 15	DR–PV integration	Coordinated DG–DR	Voltage & PV improvement	Limited CO_2 focus	Explicit coal-based CO_2 analysis
17	PV forecasting	ML-based models	Accurate prediction	No system optimization	Integrates forecast-aware optimization
19, 20	DG optimization	Metaheuristic methods	Loss & voltage improvement	Emissions ignored	Includes coal emission intensity
Proposed Work	DR–PV in coal networks	HO-based PV sizing + DR	30.79% CO_2 reduction	—	Integrated, emission-driven framework

The increasing environmental burden associated with coal-based electricity generation necessitates the exploration of strategies that can substantially curb CO_2 emissions while maintaining system reliability. Motivated by this challenge, the present study posits that the coordinated application of DR programs and the optimal allocation of solar PV units within coal-dominated power networks can lead to considerable emission reductions. Accordingly, the research pursues two principal objectives

i To formulate and evaluate methods for the optimal integration and sizing of solar PV installations aimed at reducing CO_2 emissions from coal-fired generation, and

ii To enhance PV penetration in existing coal-based infrastructures while incorporating the variability of solar resources and temporal demand fluctuations, with a parallel objective of minimizing distribution power losses.

2 Problem Statement

Minimising the reliance on electricity supplied by conventional coal-fired power plants (CPPs) is a direct and effective means of reducing system-level CO_2 emissions. To operationalize this objective within the proposed framework, the study establishes several targeted goals, foremost among them being the minimization of active power losses.

2.1 Power Loss Minimization

Minimizing power losses within a distribution network is essential for ensuring efficient power delivery and operational reliability. Losses arise inherently due to the resistive and reactive characteristics of distribution lines, leading to energy dissipation and voltage drops as electricity flows from generation sources to end-users. Reducing these losses not only enhances system performance but also contributes indirectly to emission reduction by decreasing the amount of power that must be supplied from high-carbon sources such as CPPs. In this study, power loss minimization is treated as a key optimization objective and is quantified using the formulation provided in the lterature[24].

$$£_1 = \sum_{t=1}^{24} P_{\mathrm{L}\,(t)} \quad \ldots (1)$$

$$P_{\mathrm{L}\,(t)} = \sum_{i=1}^{N} \sum_{j=1}^{N} \alpha_{ij\,(t)}\left(P_{i\,(t)}P_{J\,(t)} + Q_{i\,(t)}Q_{J\,(t)}\right) + \beta_{ij\,(t)}\left(Q_{i\,(t)}P_{j\,(t)} - P_{i\,(t)}Q_{j\,(t)}\right) \forall t \quad \ldots (2)$$

where

$$\alpha_{ij\,(t)} = r_{ij}\cos\left(\delta_{i\,(t)} - \delta_{j\,(t)}\right)/V_{i\,(t)}V_{j\,(t)} \text{ and } \beta_{ij\,(t)} = r_{ij}\sin\left(\delta_{i\,(t)} - \delta_{j\,(t)}\right)/V_{i\,(t)}V_{J\,(t)} \quad \ldots (3)$$

2.2 Managing Reverse Power Flow

DG units that produce more electricity than is needed locally are said to be engaging in reverse power flow, which feeds excess electricity back into the grid. This phenomenon may cause voltage swings and possible equipment damage, among other stability and safety issues in the distribution network (DN). Managing reverse power flow effectively is the objective having the following limitations

$$£_2 = \sum_{t=1}^{24} P_{R\,(t)} \quad \ldots (4)$$

$$P_{R\,(t)} = \begin{cases} 0, & \text{if } I_{\mathrm{G}\,(t)} \geq I_{\mathrm{S}} \\ \mathrm{Re}\left(V_{\mathrm{G}\,(t)}\, I^{*}_{\mathrm{G}\,(t)}\right) & \text{if } I_{\mathrm{G}\,(t)} < I_{\mathrm{S}}. \end{cases} \quad \ldots (5)$$

objectives to actualize the proposed framework.

2.3 Node Voltage Deviation Control

At some nodes in the power system, the difference between the actual and standard voltage levels is known as node voltage deviation. Reactive power flow, line losses, and load variations are some of the causes of voltage discrepancies. The effectiveness of the system may be affected, losses may rise, and equipment damage may result from these variations. We want to manage voltage variations in order to address this:

$$£_3 = \left(1 + \sum_{t=1}^{24} V_{D\,(t)}\right) \quad \ldots (6)$$

$$V_{D\,(t)} = \begin{cases} \left|V_{\mathrm{Min}} - V_{i\,(t)}\right| & \text{if } V_{i\,(t)} < V_{\mathrm{Min.}} \\ 0 & \text{if } V_{\mathrm{Min.}} \leq V_{i\,(t)} \leq V_{\mathrm{Max.}} \\ \ell & \text{if } V_{i(t)} > V_{\mathrm{Max.}} \end{cases} \quad \ldots (7)$$

where ℓ is the unacceptable value.

2.4 Fitness Function

It is necessary to have a fitness function that includes different objective functions with weighting elements in order to maximize these objectives.
Fitness function (Υ_1) for level 1 optimization

$$min(\Upsilon_1) = \varphi \times M \times £_3 \quad \ldots (8)$$

where $M = £_1 + £_2$ and φ is the daily to yearly conversion product.

The objective function for level 2 of the optimisation issue will be considered as follows:

$$min(\Upsilon_2) = M \times £_3 \quad \ldots (9)$$

Υ_2 is the fitness function for level 2.

2.5 Demand Response Aggregator

During periods of heightened electricity demand, the role of a Demand Response Aggregator (DRA) becomes critical in coordinating and regulating consumer energy usage. The aggregated demand reduction is subsequently traded or offered back to the grid, thereby supporting overall system stability.

DRAs contribute significantly to lowering operational costs, enhancing grid reliability, and mitigating the strain on power infrastructure during peak load conditions. By offering financial or operational incentives, they motivate consumers to reduce their consumption when the system is under stress, effectively minimizing the need for additional generation capacity. In doing so, DRAs help maintain an efficient balance between electricity supply and demand.

The key limitations associated with demand response, which require careful consideration, are summarized below,

$$P_{i(t)} = \left(P_{Gi(t)} - P_{Di(t)}\right) \forall t, i \quad \ldots (10)$$

$$Q_{i(t)} = \left(Q_{Gi(t)} - Q_{Di(t)}\right) \forall t, i \quad \ldots (11)$$

$$P_{Di(t)} = \left(P_{in,i(t)} + P_{el,i(t)}\right) \forall t, i \quad \ldots (12)$$

$$\sum_{i=1}^{N} \sum_{t=1}^{24} \left(P_{in,i(t)} + P_{el,i(t)}\right) \times \Delta t = E_i^{Total} \quad \ldots (13)$$

$$P_{el,i}^{min} \leq P_{el,i(t)} \leq min\left(\left(C - P_{in,i(t)}\right), P_{el,i}^{max}\right) \forall \quad \ldots (14)$$

$$P_{el,i}^{max} = \mu \sum_{t=1}^{24} L_{d,i(t)} \quad \ldots (15)$$

where C and μ is the contract load and DR penetration rate respectively.

2.6 Objective Constraints

These objective functions are subject to constraints to account for technical and operational considerations

2.6.1 Solar PV Output Constraint

$$0 \leq P_{\mathrm{DG},i} \leq P_{DG}^{max} \forall i \quad \ldots (16)$$

2.6.2 Feeder Thermal Limits Constraint

$$I_{ij(t)} \leq I_{ij}^{max} \forall t, i, j \quad \ldots (17)$$

2.6.3 Real Power and Reactive Power Constraints

$$P_{i(t)} = V_{i(t)} \sum_{j=1}^{N} V_{j(t)} Y_{ij} \cos\left(\theta_{ij} + \delta_{j(t)} - \delta_{i(t)}\right) \forall t, i \quad \ldots (18)$$

$$Q_{i(t)} = -V_{i(t)} \sum_{j=1}^{N} V_{j(t)} Y_{ij} \sin\left(\theta_{ij} + \delta_{j(t)} - \delta_{i(t)}\right) \forall t, i \quad \ldots (19)$$

2.7 Modeling of Demand

Demand modeling is expressed as

$$P_{D,i(t)} = \Omega_{i(t)} P_{D,i}^{0} \forall t, i \quad \ldots (19)$$

$$Q_{D,i(t)} = \Omega_{i(t)} Q_{D,i}^{0} \forall t, i \quad \ldots (20)$$

where $\Omega_{i(t)}$ is the assigned load factor for the time period t.

2.8 Modeling of Solar PV Output

A number of variables, including solar radiation, tilt angle, and solar panel properties, affect the production of solar power. The calculation of the current in relation to the rated voltage, assuming that all other factors stay same over the designated time, is as follows

$$I_{sm(t)} = \begin{cases} I_{sm} \text{ if } S_{r(t)} \geq S_r^r \\ I_{sm} \times S_{r(t)}/S_r^r \text{ if } S_{r(t)} < S_r^r \end{cases} \quad \ldots (21)$$

In conclusion, there are several goals covered by this study framework, ranging from managing reverse power flow and reducing power loss to regulating node voltage deviation. A fitness function with weighted elements is used to maximize these goals. Furthermore, emphasis is placed on the DRA's function in controlling peak energy usage. Demand and solar PV output are also modeled to aid in the optimization process, and the framework complies with a number of restrictions to guarantee that technical and operational factors are satisfied.

3 Optimization Method

The HO algorithm is a recently developed nature-inspired metaheuristic that models the collective foraging, territorial behavior, and adaptive movement patterns of hippopotamuses in natural ecosystems. As a population-based stochastic optimizer, HO aims to achieve an effective balance between global exploration and local exploitation, making it suitable for addressing complex nonlinear optimization problems in engineering and computational domains.

The algorithm begins by initializing a population of hippo agents randomly within the defined search bounds. During the exploration phase, agents perform large-step stochastic movements to survey wide regions of the search space, guided by environmental variability and the global best solution. Once

promising regions are identified, the algorithm shifts to the exploitation phase, where hippos intensify their search locally through competitive territorial behavior, progressively converging toward high-fitness regions. An adaptive migration mechanism further refines the search by dynamically adjusting movement intensity, facilitating a smooth transition from exploration to exploitation.

Fitness evaluation and iterative selection ensure that superior solutions are retained across generations, enabling efficient convergence. Due to its simplicity, strong global search capability, and robust convergence characteristics, HO has emerged as an effective optimization tool for applications such as renewable energy scheduling, distributed generation management, machine learning tuning, and multi-objective engineering design[25]. For the quick overview of HO technique, a process model is shown in Fig. 1.

After a thorough literature study, these criteria were chosen, with particular reference to the work of various researcher[26-30]. Both Level-1 and Level-2 optimization problems are customized to meet their unique requirements and features. The parameters selected are meant to effectively converge to high-quality solutions while staying within the allocated computational resources. The flow chart of the proposed technique is demonstrated in Fig. 2. Table 2 presents the optimization parameters for the implementation of the proposed approach at level 1 and level 2.

Fig. 1 — Hippopotamus Optimization

4 Test System

This study's multilevel optimization method will be used on the IEEE 33 bus system as shown in Fig. 3. The grid's power supply will come from the Indian CPP. A comprehensive examination and analysis of the impacts of DR technology is the focus of this study. The objective is to identify the best power transmission techniques while taking into account a variety of circumstances and limitations. The main objective is to increase power distribution efficiency. The implementation of the proposed optimization methodologies will be carried out using MATLAB software. Table 3 presents the values of system parameter during the implementation of proposed approach.

5 Results and Discussion

5.1 Base Case

The Base Case represents system operation without any DG or DR interventions. The network experiences the highest maximum demand of 6519 kW and a daily demand of 73,474 kWh, resulting in high daily losses (3906.84 kWh) and annual losses of 1426 MWh. The average voltage level remains relatively low at 0.978 p.u., indicating voltage stress during peak loading. As expected, this case yields the maximum CO_2 emissions (75,446.33 kg/day) since the entire energy requirement is met by the CPP. These observations establish the baseline against which all other cases are compared. Tables 4-6 present the demand distribution, performance assessment, and the impact on CO_2 reduction following the implementation of the proposed approach.

Table 2 — Simulation Parameters for HO Algorithm

Parameters	Level-1	Level-2
Population Size	30	60
Exploration Coefficient (α)	1.2	1.8
Exploitation Coefficient (β)	0.6	0.9
Adaptive Movement Factor (γ)	0.4	0.2
Maximum Iterations	80	120

5.2 DG Only

Introducing DG significantly transforms system behaviour. Although maximum demand remains unchanged, DG injection at three optimal buses sharply reduces daily demand to 50,047 kWh, owing to local generation support. This results in a notable 22.89 % annual loss reduction and an increase in the average voltage to 0.999 p.u., demonstrating improved voltage stability. The DG system achieves high PV utilization (72.91 %), reflecting effective renewable penetration. CO_2 emissions decline substantially by 27.84 %, as DG displaces CPP generation. Overall, this case highlights the strong impact of DG on reducing losses, improving voltage profiles, and lowering emissions, even without DR participation. The effect of DG allocation on demand, voltage level, and power losses are shown in Figs. 4-6, respectively.

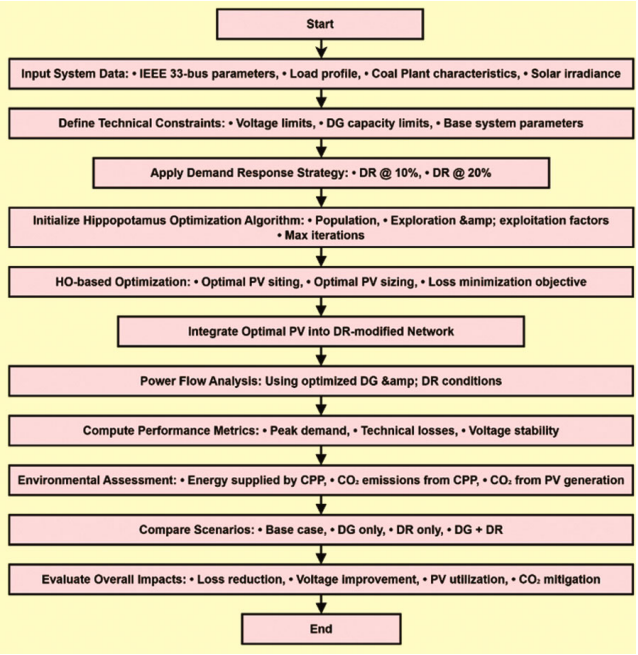

Fig. 2 — Methodological Diagram for the proposed approach

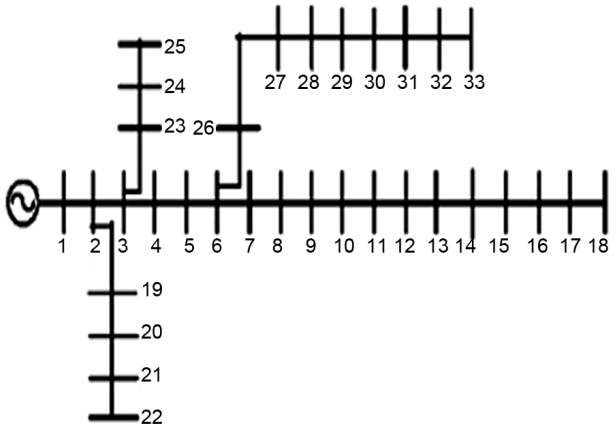

Fig. 3 — IEEE 33 bus system[31]

5.3 DR at 10 %

Applying 10 % DR reduces the maximum demand by 18.98 %, from 6519 kW to 5281.34 kW. This contributes to a 6.26 % reduction in annual losses and a decrease in the daily demand span. However, since no DG is present, CPP remains the sole energy provider, resulting in only marginal CO_2 reduction (0.32 %) due to shifts in demand rather than displacement of fossil-based energy. Average voltage improves only slightly. This case demonstrates that DR alone helps mitigate peak demand and losses but has limited influence on emission reduction. The effect of 10 % DR rate on demand, and power losses are shown in Figs. 7-8, respectively.

5.4 DR at 20 %

With a higher DR capacity, maximum demand drops to 5058.47 kW, a reduction of 22.41 %, with further improvement in demand span and loss mitigation (8.61 %). Daily losses reduce to 3407.99 kWh, reflecting improved system performance. Still, because there is no DG support, overall CO_2 reduction remains small (0.53 %). This case confirms that DR has diminishing returns on emissions when used without DG, though it continues to benefit peak shaving and loss reduction. The effect of 20 % DR rate on demand, and power losses are shown in Figs. 9 and 10, respectively.

Table 3 — System parameters used for the optimization process

Parameter	Value	Unit	Description
Base Voltage	12.66	kV	Rated line voltage of the distribution system
Nominal Active Demand	3715	kW	Total system active power demand
Nominal Reactive Demand	2300	kVAR	Total system reactive power demand
Power Loss (Base Case)	202.7	kW	Real power losses in the initial operating state
Minimum Voltage (V_{min})	0.95	p.u.	Lower acceptable voltage limit
Maximum Voltage (V_{max})	1.05	p.u.	Upper acceptable voltage limit
Maximum DG Capacity (P_{DG}^{max})	2.0	MW	Maximum allowable distributed generation per unit

Table 4 — Demand distribution after implementation of proposed approach

Case No.	Type of Case	Maximum Demand (kW)	Reduction in Maximum Demand (%)	Demand Span (kW)	% of Maximum Loss Mitigation at 20:00 h
5.1	Base Case	6519.00	—	5397.73	—
5.2	DG only	6519.00	—	6016.39	—
5.3	DR @ 10 %	5281.34	18.98	3957.83	26.77
5.4	DR @ 20 %	5058.47	22.41	3543.07	32.52
5.5	DG + DR @ 10 %	5107.88	21.65	4106.73	31.30
5.6	DG + DR @ 20 %	4554.84	30.12	3363.30	44.42

Table 5 — Performance Assessment of Different Operational Cases With DR and Optimally Integrated DG

Case No.	Type of Case	DG Location (Bus No., kW)	Demand/Day (kWh)	Yearly Losses (MWh)	Losses/Day (kWh)	Loss Reduction/Year (%)	PV Utilization (%)	Avg. Voltage (p.u.)
5.1	Base Case	–	73474	1426	3906.84	–	–	0.978
5.2	DG	14(1343)-30(1706)-25(1078)	50047	1059.25	2902.05	22.89	72.91	0.999
5.3	DR @ 10 %	–	69798	1273.95	3490.27	6.26	–	0.979
5.4	DR @ 20 %	–	69705	1243.55	3407.99	8.61	–	0.979
5.5	DG + DR @ 10 %	15(1163)-7(1876)-33(904)	48150	961.40	2633.00	30.48	69.65	0.999
5.6	DG + DR @ 20 %	18(418)-29(1820)-11(1636)	51773	903.45	2475.20	34.98	67.79	

Table 6 — Impact of Coordinated Demand Response and Optimally Integrated DG on Energy Requirements and CO_2 Emissions

Case	Type of Case	Energy Required from CPP (kWh/day)	Energy Supplied by DG (kWh/day)	CO_2 Emissions from PV (kg/day)	Energy Losses / Day (kWh)	Total Energy Delivered by CPP (kWh/day)	CO_2 Emissions from CPP (kg/day)	Total CO_2 Emissions (kg/day)	CO_2 Reduction (%) /Day
5.1	Base Case	73,474.00	—	—	3,906.85	77,380.85	75,446.33	75,446.33	—
5.2	DG	50,046.95	21,832.65	1,046.93	2,902.05	52,949.00	51,625.28	52,671.21	27.84
5.3	DR @ 10 %	69,798.40	—	—	3,490.27	73,388.67	71,456.45	71,456.45	0.32
5.4	DR @ 20 %	69,740.45	—	—	3,406.99	73,147.44	71,318.75	71,318.75	0.53
5.5	DG + DR @ 10 %	48,149.80	23,929.50	1,147.48	2,633.00	50,783.77	49,514.18	50,661.66	30.79
5.6	DG + DR @ 20 %	51,723.10	19,924.80	955.44	2,475.21	54,248.31	52,892.10	53,84	26.11

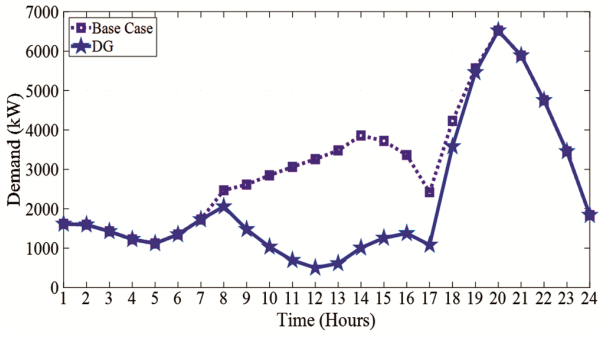

Fig. 4 — Level of demand during 24 hrs of a day after DG allocation

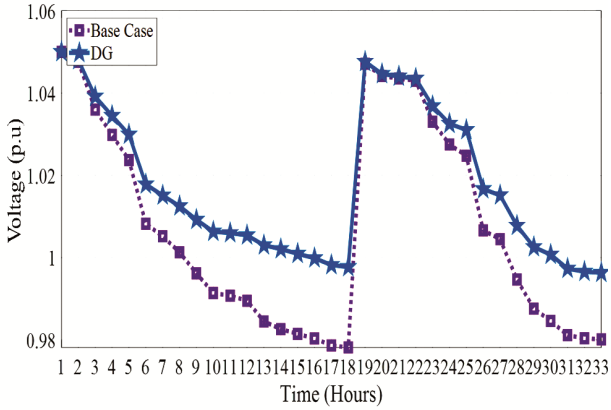

Fig. 5 — Level of voltage at 33 nodes after DG allocation

5.5 DG + DR @ 10 %

Combining DG with 10 % DR results in synergistic improvements. Maximum demand decreases to 5107.88 kW, while DG generation reduces fossil fuel reliance considerably. The system achieves a 30.48 % annual loss reduction, and the voltage reaches 0.999 p.u., indicating a robust voltage profile. Daily demand drops to 48,150 kWh, the lowest among all cases. CO_2 emissions decline by 30.79 %, surpassing all previous cases. This synergy demonstrates that combining DR with DG maximizes both operational and

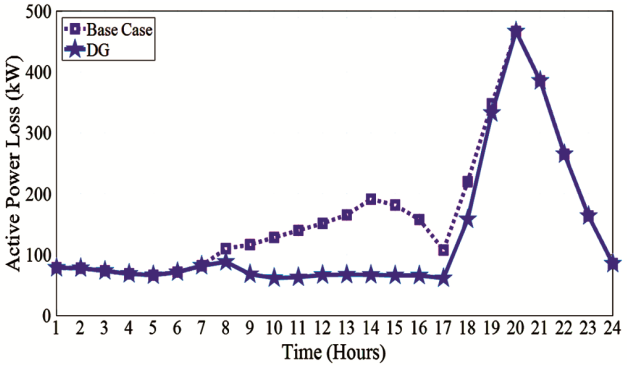

Fig. 6 — Active power losses during 24 hrs of a day after DG allocation

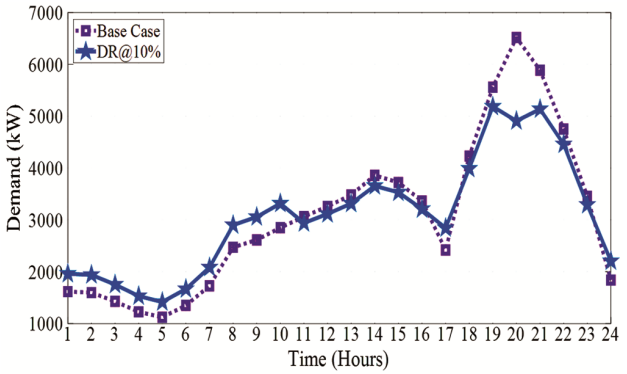

Fig. 7 — Level of demand during 24 hrs of a day after 10 % DR

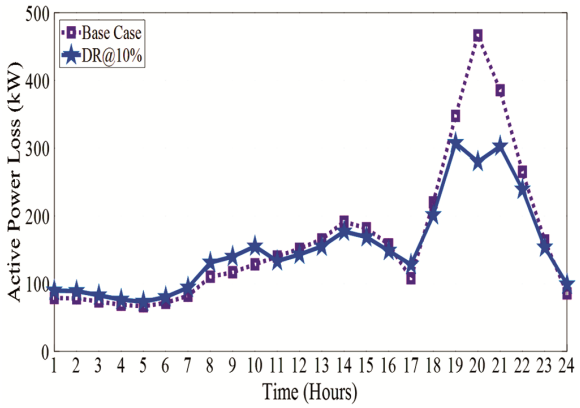

Fig. 8 — Active Power losses during 24 hrs of a day after 10 % DR

environmental benefits. The effect of DG allocation with 10 % DR rate on demand, voltage level, and power losses are shown in Figs. 11-13, respectively.

5.6 DG + DR @ 20 %

This is the best-performing scenario overall. Maximum demand drops to 4554.84 kW, representing the largest reduction (30.12 %). The system demonstrates 34.98 % annual loss reduction, the highest among all cases. DG penetration remains

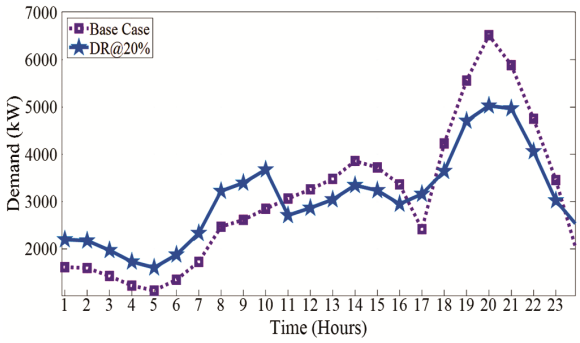

Fig. 9 — Level of demand during 24 hrs of a day after 20 % DR

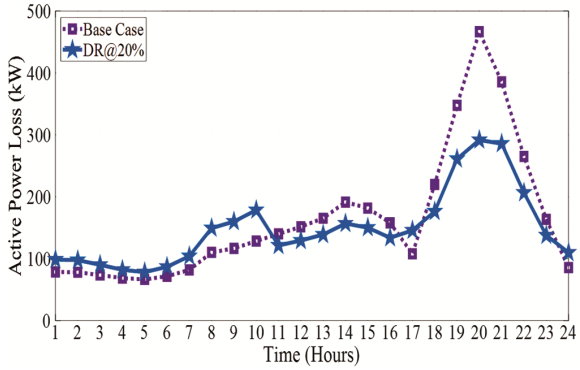

Fig. 10 — Active power losses during 24 hrs of a day after 20 % DR

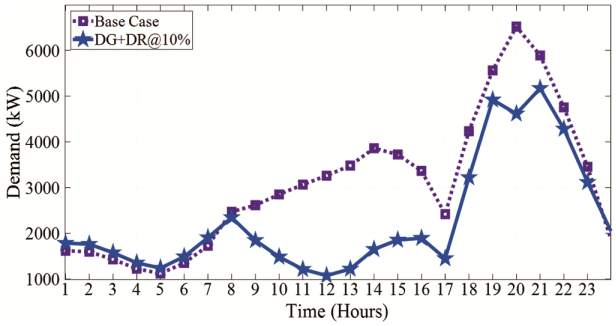

Fig. 11 — Level of demand during 24 hrs of a day after DG allocation and 10 % DR

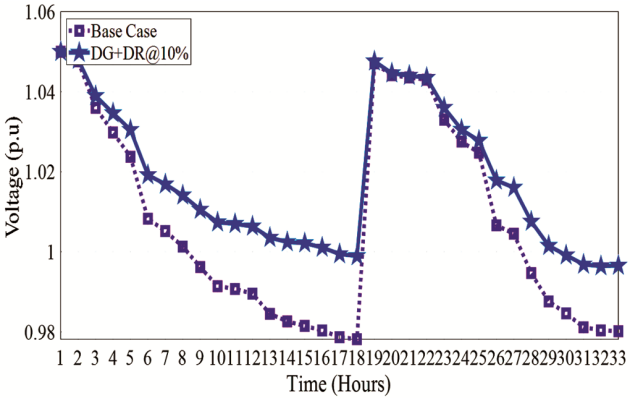

Fig. 12 — Level of voltage at 33 nodes after DG allocation and 10 % DR

strong, though PV utilization slightly decreases due to greater DR-induced load reduction. Voltage stability is maintained at 0.999 p.u. CO_2 emissions drop significantly (≈28%–29 % depending on rounding), rivalling in this case, though slightly lower DG utilization leads to a mild dip in emission reduction compared to previous case (DG + DR@10 %). This case emphasizes that high DR participation, coupled with optimally placed DG, provides the most substantial improvements in demand management, loss reduction, and voltage stability. The effect of DG allocation with 20 % DR rate on demand, voltage level, and power losses are shown in Fig. 14-16, respectively. Further a comparative illustration is shown in Fig. 17 for the impact on various parameters after the integration of the different categories.

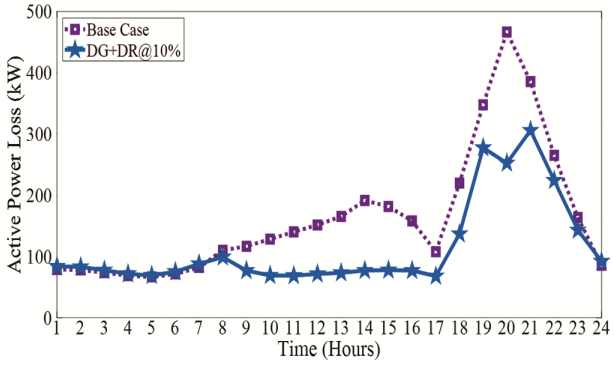

Fig. 13 — Active power losses during 24 hrs of a day after DG allocation and 10 % DR

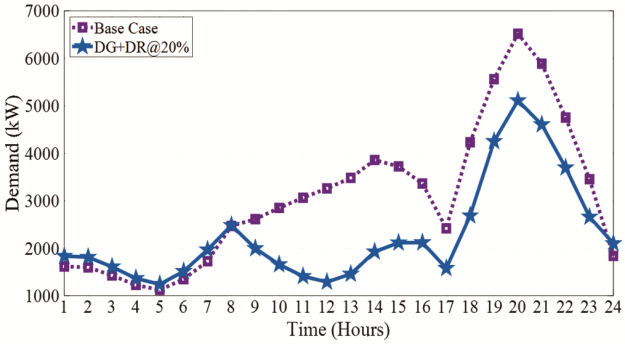

Fig. 14 — Level of demand during 24 hrs of a day after DG allocation and 20 % DR

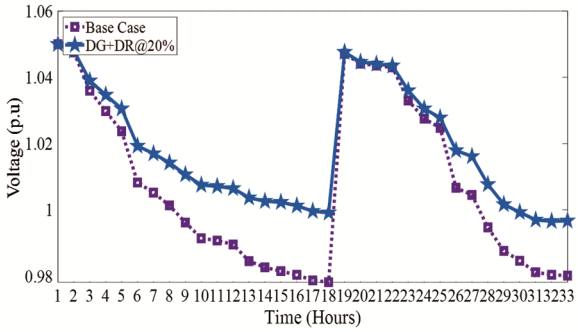

Fig. 15 — Level of voltage at 33 nodes after DG allocation and 20 % DR

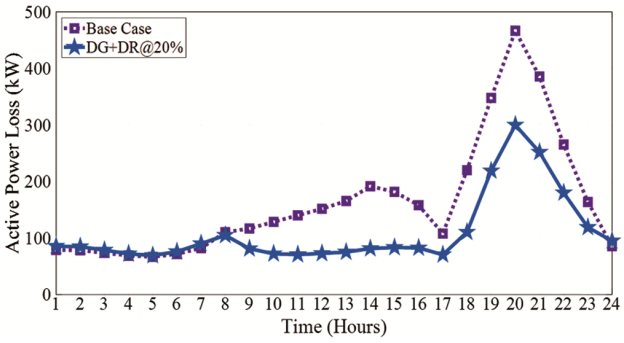

Fig. 16 — Active power losses during 24 hrs of a day after DG allocation and 20 % DR

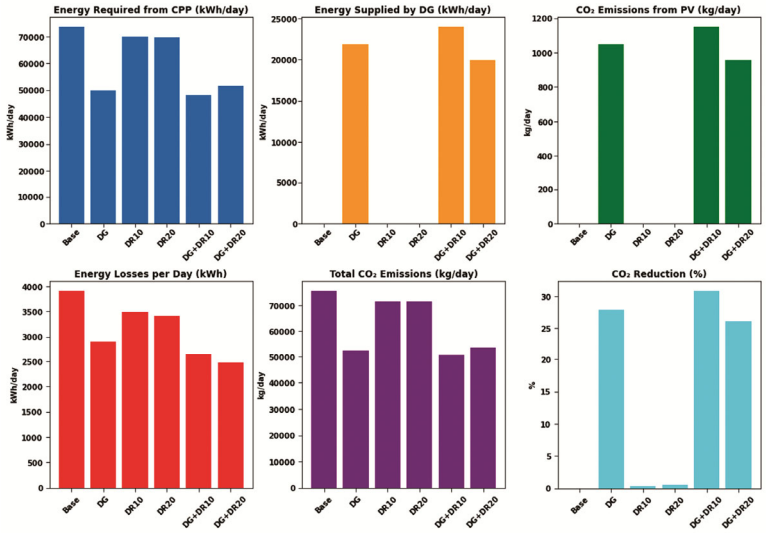

Fig.17 — Comparative illustration of various parameters after implementation of proposed approach

6 Conclusion

The comparative evaluation of all operational scenarios demonstrates the distinct and combined impacts of demand response and optimally integrated solar PV on system performance and emissions within a coal-dominated distribution network.

First, demand response alone provides measurable operational benefits, particularly in reducing peak demand and alleviating network loading. DR@10–20 % lowers peak demand by approximately 19–22 % and decreases daily losses. However, because coal-based generation continues to supply nearly the entire energy requirement, its influence on CO_2 emissions remains negligible (<1 %). Thus, DR is effective for load management but has limited decarbonization potential when deployed in isolation.

Second, optimally sited and sized distributed PV generation significantly enhances system efficiency. DG integration reduces yearly losses by nearly 23 %, improves the average voltage profile to nearly 1.0 p.u., and achieves a substantial reduction in CO_2 emissions of about 28 %. These improvements directly result from the displacement of coal-fired generation, demonstrating that renewable penetration is the primary driver of emission mitigation.

Third, the coordinated deployment of DG and DR yields the most favorable outcomes across all evaluation metrics. The combined DG + DR scenarios deliver the highest peak demand reduction (up to 30 %), the largest loss reduction (≈35 %), and the strongest improvement in voltage stability. Moreover, the joint strategy achieves the maximum CO_2 reduction of 30.79 %, highlighting the synergistic benefits of integrating supply-side renewable generation with demand-side flexibility.

Although higher levels of DR slightly reduce PV utilization as demand curtailment lowers the energy absorption capability of the system this does not offset the overall operational or environmental gains. The findings suggest that complementary measures such as energy storage or advanced DR scheduling could further enhance renewable utilization.

Overall, the results confirm that coordinated DR–PV integration is a highly effective pathway for technical enhancement and substantial decarbonization in coal-reliant distribution systems, offering a robust framework for policy and planning in transitioning power sectors.

Abbreviations

$P_{\mathrm{L}\,(t)}$	Power transmission losses
$P_{i\,(t)}$	Real power at ith node at any time t
$P_{J\,(t)}$	Real power at jth node at any time t
$Q_{i\,(t)}$	Reactive power at ith node at any time t
$Q_{J\,(t)}$	Reactive power at jth node at any time t
$V_{i\,(t)}$	Voltage at ith node at any time t
$V_{J\,(t)}$	Voltage at jth node at any time t
r_{ij}	resistance of branch between ith and jth node
$\delta_{i\,(t)}$	Angle of voltage at ith node
$\delta_{j\,(t)}$	Angle of voltage at jth node
$P_{R\,(t)}$	Reverse power at time t
$I_{\mathrm{G}\,(t)}$	Current from grid at time t
$V_{\mathrm{G}\,(t)}$	Voltage of grid at time t
$I_{\mathrm{S.}}$	Designated limit of reverse current
$V_{D\,(t)}$	Penalty for deviation of voltage
$V_{\mathrm{Max.}}$	Maximum value of permissible voltage at node
V_{Min}	Minimum value of permissible voltage at node
$P_{Gi(t)}$	Real power generation at ith node for the time period t
$P_{Di(t)}$	Real power demand for the time period t
$Q_{Gi(t)}$	Reactive power generation at ith node for the time period t
$Q_{Di(t)}$	Reactive power demand for the time period t
$P_{in,i(t)}$	Nonreceptive load at time t
$P_{el,i(t)}$	Receptive load at time t
E_i^{Total}	Energy demand per day
$L_{d,i(t)}$	Load per hour for the time period t
$P_{\mathrm{DG},i}$	Real power injection by DG
P_{DG}^{max}	Maximum value of real power generation by DG
$I_{ij(t)}$	Current flowing between ith and jth Node at t
I_{ij}^{max}	Maximum permissible value of current
Y_{ij}	Admittance matrix between ith and jth Node
θ_{ij}	Angle of impedance between ith and jth Node
I_{sm}	Current of solar PV
$S_{r(t)}$	Solar radiation at t
S_r^r	Rated value of solar radiation for PV

References

1 Kumar P, Yadav AK, Jha SK, *et al.*, *MAPAN J Metrol Soc India*, 40 (2025) 629.

2 Saxena V, *MAPAN J Metrol Soc India*, 40 (2025) 1007.

3 Saxena V, Manna S, Rajput S K, Kumar P, Sharma B, Alsharif M H & Kim M K, *Energy Rep*, 12 (2024) 3302.

4 Saxena V, Manna S, Rajput S K, Sharma B, Kumar P, Diwania S, Gupta V, Alsharif M H & Kim M K, *Energy Rep*, 13 (2025) 6450.

5 Cheng D, *et al*., *Int Confer Smart Electrical Grid and Renewable Energy (SEGRE)*, Changsha, China, 16-19 June 2023.

6 Ma L, *et al*., *4th Int Confer Electrical Engineering and Control Technologies (CEECT)*, Shanghai, China, 16-18 December 2022.

7 Samanta S & Ghosh S, *Energy Procedia*, 90, (2015) 456.

8 Zhang L, Li J, Tian Y & Cheng Y, *J Clean Product*, 242 (2020) 118518.

9 Smaisim G F, Abed A M, Alavi H, *Int J Low-Carbon Technol*, 18 (2023) 38.

10 Eslami M, Shareef H & Mohamed A, *Int Rev Electr Eng*, 6 (4) (2011) 1984.
11 Hanak D P, Biliyok C & Manovic V, *Appl Energy*, 151, (2015) 258.
12 Yaghoubi M, *et al*., *IEEE Access*, 10, (2022) 110181.
13 Saxena V, Kumar N & Nangia U, *J Phys Conf Ser*, 1 (2021) 012042.
14 Saxena V, Kumar N & Nangia U, *Artif Intell Sustain Comp*, (2022) 33-46.
15 Eslami M, Shareef H, Mohamed A & Khajehzadeh M, *Przegl Elektrotech*, 88 (1A), (2012) 1.
16 Zhong X, Heping P, Wenxiong M, Yong W & Le L, Int Confer Power Syst Technol (POWERCON) Haikou, China, 2021 p.1105-1110.
17 Al-Ghussain L, *et al*. Energy Sources, *Part A Recovery, Utilization, Environ Effects*, 45 (1) (2023) 523.
18 Viana M S, Manassero G & Udaeta M E M, *Appl Energy*, 217 (2018) 456.
19 Shirazi H, Ghiasi M, Dehghani M, Niknam T, Garpachi M G & Ramezani A, 7th Int Conf Control, Instrumentation and Automation (ICCIA) Tabriz, Iran, 2021 p. 1-6.
20 Wang X, Huang G, Qiao Z & Li X, IEEE Sustain Power Energy Conference (iSPEC) Nanjing, China, 2021 p. 2101-2107.
21 Lakshmi G V N, Jayalaxmi A & Veeramsetty V, *Electr Eng*, 105 (2023) 965.
22 Central Electricity Authority (CEA), *CO_2 Emission from Power Sector in India during 2021–22*, Ministry of Power, Govt of India, New Delhi, 2023.
23 Rajput S K & Dheer D K, *Int J Ambient Energy*, 1 (2022) 8176.
24 Meena N K, Parashar S, Swarnkar A, Gupta N & Niazi K R, *IEEE Trans Industr Inf*, 14 (3) (2018) 1029.
25 Saxena V, Kumar N & Nangia U, *Lect Notes Electr Eng*, 721 (2021) 735.
26 Saxena V, Kumar N, Nangia U, *Arch Comput Methods Eng*, 30 (2023) 675.
27 Saxena V, Kumar N & Nangia U, *Ing Investig*, 42 (3) (2022) 97702.
28 Saxena V, Kumar N & Nangia U, *Arch Comput Methods Eng*, 31, (2024) 2385.
29 Saxena V, Rajput S K, Manna S, Gantayet A, Agarwal K L, Alsharif M H & Kim M K *Energy Rep*, 15 (2026) 108882.
30 Amiri M H, Hashjin, N M, Montazeri M, *et al.*, *Sci Rep*, 14 (2024) 5032.
31 Baran M E & Wu F F, *IEEE Trans Power Deliv*, 4 (2) (1989) 1401.